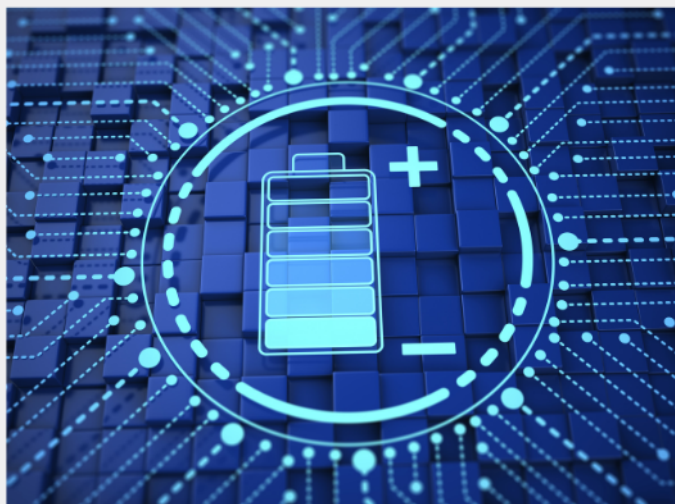# Exploring the possibilities of increasing energy density and efficiency in rechargeable batteries

Download this complimentary article collection

The exponential rise in the need for better, more efficient power sources has sparked an incredible amount of research into batteries. A primary focus of research has been increasing the energy density of batteries, as it allows for lighter, more portable storage of energy. Lithium-ion batteries, for example, have a much higher energy density than conventional lead-acid batteries and can be used for various purposes, such as in electric vehicles.

This article collection provides a comprehensive list of references for new methods and technologies for increasing the energy density of batteries.

Metrohm

WILEY

RESEARCH ARTICLE

ADVANCED
FUNCTIONAL
MATERIALS
www.afm-journal.de

Check for updates

Selective Peptide Binders to the Perfluorinated Sulfonic Acid Ionomer Nafion

Dimitry Schmidt, Patrizia Gartner,* Ivan Berezkin, Jens Rudat, Maximilian Bilger, Tom Grünert, Nadine Zimmerer, Philipp Quarz, Philip Scharfer, Julian Brückel, André P. Jung, Pooja Singh, Pooja Pooja, Benno Meier, Mareen Stahlberger, Wilhelm Schabel, Stefan Bräse, Gisela Lanza, and Alexander Nesterov-Mueller*

Fuel cells used for transport applications hold polymer membranes as a key element. Their efficiency can be significantly increased if structured ion channels are implemented at the molecular level into the proton-conducting membrane. New functional molecules with selective affinity for ionomers are needed to obtain such a membrane design. This study presents a method to screen for selective peptide binders to perfluorinated sulfonic acid ionomers, e.g., Nafion using ultra-high density peptide arrays with a spot size of up to 30 µm. First, the ionomer dispersion is incubated with the peptide chip containing 56014 randomly chosen 6-mer peptides. Afterward, the peptide chip is washed. The peptide WIWHCW with the helix structure is identified as a selective binder to Nafion. The invariant amino acids responsible for binding are also determined using a peptide chip approach. The specific binding pocket of WIWHCW is formed by histidine and tryptophan. Its dissociation constant to the ionomer is measured at ≈140 µM.

1. Introduction

Polymer electrolyte membrane fuel cells (PEM-FC) offer a promising approach for a wide range of applications, including long-distance and heavy-duty vehicle propulsion and decentralized stationary energy systems, to achieve ambitious energy transition goals.[1] The heart of the PEM-FC is the so-called catalyst-coated membrane (CCM), in which energy-converting reactions occur. The CCM comprises a polymer membrane coated with a catalyst layer on both sides. The interface between the catalyst layer and the membrane is particularly important for the performance and durability of the fuel cell.[2] The perfluorinated sulfonic acid polymer membrane Nafion (a trademark polymer from DuPont) is the most widely used membrane material in state-of-the-art fuel cells.[3]

Various possibilities are being investigated to improve the performance of the fuel cell by modifying the membrane/catalyst interface: composite membranes made by infiltrating Nafion in polytetrafluoroethylene fibrous substrates,[3] carbon nanofibers as catalyst supports with subsequent optimization of the ionomer content,[4] special 3D shapes of catalysts

D. Schmidt, I. Berezkin, M. Stahlberger, A. Nesterov-Mueller
Institute of Microstructure Technology (KIT)
Karlsruhe Institute of Technology
Hermann-von-Helmholtz-Platz 1, 76344 Eggenstein-Leopoldshafen, Germany
E-mail: alexander.nesterov-mueller@kit.edu

P. Gartner, G. Lanza
Institute of Production Science
Karlsruhe Institute of Technology
Kaiserstr.12, 76131 Karlsruhe, Germany
E-mail: patrizia.gartner@kit.edu

The ORCID identification number(s) for the author(s) of this article can be found under https://doi.org/10.1002/adfm.202214932.

J. Rudat, M. Bilger, T. Grünert
Institute of Process Engineering in Life Sciences 2: Technical Biology
Karlsruhe Institute of Technology
Kaiserstr.12, 76131 Karlsruhe, Germany

N. Zimmerer, P. Quarz, P. Scharfer, W. Schabel
Thin Film Technology
Karlsruhe Institute of Technology
Kaiserstr.12, 76131 Karlsruhe, Germany

J. Brückel, A. P. Jung, S. Bräse
Institute of Biological and Chemical Systems
Karlsruhe Institute of Technology
Hermann-von-Helmholtz-Platz 1, 76344 Eggenstein-Leopoldshafen, Germany

P. Singh, P. Pooja, B. Meier
Institute for Biological Interfaces 4
Karlsruhe Institute of Technology
Hermann-von-Helmholtz-Platz 1, 76344 Eggenstein-Leopoldshafen, Germany

mostly from platinum alloys to enable uniform distribution of ionomers.[5] Recently, new concepts have been proposed to improve the mass transfer of the membrane electrode assembly (MEA) by structuring ion channels at the molecular level.[6] In particular, it has been shown that a membrane with proton-transport channels oriented perpendicular to the membrane/electrode surface enables efficient proton conduction even at an extremely low relative humidity.[7] However, to exploit the great potential of such a structural approach, new functional molecules are needed that selectively can bind to the Nafion ionomer. Peptides could be promising templates for this task. Bioconjugates are not new in the field of energy storage and conversion materials. For instance, Ki Tae Nam et al. integrated the binding peptide motif into the coat proteins of bacteriophages to assemble nanowires from metal oxides as negative electrode materials for Li-ion batteries.[8] We propose a method to screen for peptide binders to an ionomer according to the lock-and-key principle.[9] Such binding, well known for antibodies, is accompanied by a stable ligand orientation to the trapping molecule. This kind of binding is especially useful because the ionomer does not need to be chemically modified. Peptides from amino acids with different functional side groups can have many additional functionalities for developing proton-transport-oriented membranes. Tailored peptides form stable nanotubes[10] or nanospheres,[11] have chemical stability at temperatures of >90 °C if embedded in polymers,[12] determine the film pattern after solvent evaporation,[13] and join Nafion with the gold electrode through the side group of lysine and a cysteine residue.[14]

Previously, peptides up to 12 amino acids in length have been reported to adhere to metal and metal oxide surfaces selectively[15] as well as semiconductors.[16] These peptides were screened using combinatorial phage-display libraries to develop novel heterojunctions for electronic devices and lithium-ion batteries.[8]

However, the use of phage display,[17] as well as other recombinant display techniques such as ribosome display[18] or cDNA display,[19] makes it difficult to search for specific hydrophobic binders. Sequences with hydrophobic amino acids possess propagation disadvantages due to their stickiness to surfaces and are not considered in the following panning rounds.[20]

Nafion is a copolymer consisting of a hydrophobic tetrafluoroethylene main chain and, in addition, perfluoroalkyl ether side chains that end with a hydrophilic sulfonyl group.[21] Due to this chemical structure, hydrophobic bonds play a significant role in interacting with Nafion. A strong adhesion of Nafion on hydrophobic surfaces was reported, in which the fluorocarbon backbone was responsible for the strong binding, and the sulfonic acid groups of the ionomer were oriented outward.[22] In contrast to recombinant screening methods, ultra-high density peptide arrays have been successfully used to screen for hydrophobic peptides as off-target specific binders to therapeutic antibodies.[23]

In this work, we use ultra-high density peptide arrays to screen for optimal selective peptide binders for an ionomer dissolved in solution, perform a substitutional analysis of the found sequences, evaluate their dissociation constants, and study the deposition of the selected hydrophobic peptide on the Nafion membrane.

2. Results and Discussion

2.1. Peptide Library and Screening for Peptide Binders

A peptide library containing 56014 randomly selected 6-mer peptides was used for the initial screening. Each peptide was represented by a triplet. These initial and other substitution peptide libraries (**Figure 1**) were synthesized on ultra-high density peptide microarrays (axxelera UG, Karlsruhe, Germany). The entire initial library fits on a conventional microscope slide 75 mm × 25 mm. The spot size and the distance between the spots were 30 µm. The peptides were randomly distributed over the spots to exclude the influence of local effects on the measuring pixel interactions with ionomer dispersion. Nafion dispersion (B2020CS, Fuel Cell Store, Pinon Drive, TX, USA) with ionomer concentration of 0,22 mmol Ml^{-1} was diluted 1:10 in ethanol and incubated with the peptide library at 140 rpm and room temperature for 12 h. After incubation with the Nafion dispersion, the peptide chip was scanned on a confocal fluorescent scanner Innoscan 1100 AL (Innopsys, Carbonne, France). The ionomer molecules on peptide spots were detected via excitation of Nafion autofluorescence at a wavelength of 532 nm. The scans were performed with a resolution of 2 µm. Photometric parameters for each sequence on the peptide chip were determined using Mapix software (Innopsys, Carbonne, France) based on a fluorescence scan.

For further analysis, a single WIWHCW peptide was selected, all three copies of which showed homogenous intensity and appeared in the first 50 spots with the maximum fluorescence intensity. Other peptide binder candidates did not exhibit such performance. According to the protein database UniProt,[24] this peptide was previously identified in several lower animals, particularly in the nematode *Wuchereria bancrofti*, as part of the phosphoglucomutase/phosphomannomutase domain-containing protein J9F1D0.

2.2. Substitution Peptide Library and Dilution Experiments

The substitution library included peptides representing substitutions for the sequence WIWHCW. Substitutions for WIWHCW consisted of replacing each amino acid in the sequence WIWHCW with other amino acids. Each peptide of the new library was represented by six copies.

This substitutional library fits in one of the wells of the incubation tray shown in Figure 1a. The same substitutional library was synthesized in all eight wells within the area marked with a red dotted line. The Nafion dispersion was stepwise diluted in ethanol: 1:2, 1:4, 1:8, 1:16, 1:32, 1:64, 1:128, and 1:256. Each diluted sample was incubated with the substitutional peptide library at 140 rpm and room temperature for 12 h. As in the previous experiment, an Innoscan 1100 AL confocal fluorescence scanner was used to identify the fluorescence signals from the spots (Figure 1b,c).

Figure 1d shows profiles of the ionomer films on different peptide spots measured with a vertical scanning interferometer (Bruker, Karlsruhe, Germany). The thickness of Nafion film on the spot does not exceed 2.0 nm. Previously, it was shown that the thickness of ligands accumulated on peptide spots
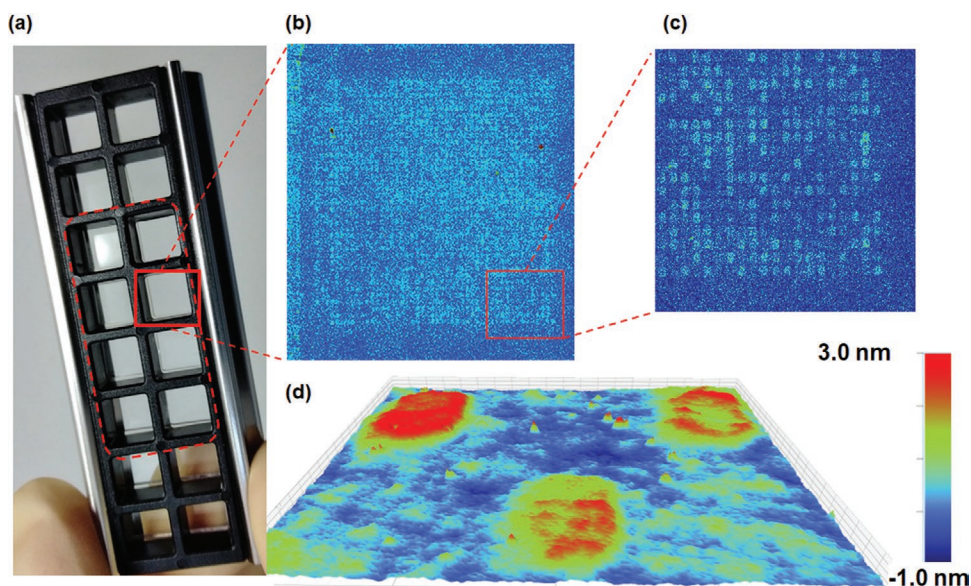
Figure 1. Alignment of the eight identical peptide libraries for substitution analysis and measurement of dissociation constants. a) Photo of a peptide chip in the incubation tray. The eight wells in the middle (dashed red line) were used to incubate the Nafion ionomer at eight concentrations to determine the dissociation constant. b and c) A fragment of fluorescence images of peptide libraries after incubation and its magnification. d) Profiles of the ionomer film accumulated on six peptide spots with different affinity to Nafion measured with a vertical scanning interferometer (three of the spots had no Nafion adhesion). The ionomer thickness on the peptide spot with the highest affinity (upper left corner) is <2 nm). The surface roughness of the peptide chip is ≈1.5 nm.

measured with a vertical scanning interferometer corresponds to the thickness obtained with an atomic force microscope.[25] The local inhomogeneity of the optical profiles within one spot corresponded to the surface roughness of the polymer layer on which the peptides were synthesized.

Figure 2 shows the substitution array for the WIWHCW peptide. It demonstrates the significant role of histidine (H, His), replacing that with other amino acids significantly reduced the binding strength to the ionomer. Also, the replacement of tryptophan (W, Trp) in the sequence next to histidine reduces the strength of the fluorescent signal. At the same time, replacing cysteine (C, Cys) and isoleucine (I, Ile) with other amino acids does not significantly affect the interaction between the ionomer and the peptide.

To more clearly represent this result, we used the 3D structure of WIWHCW (**Figure 3**). WIWHCW forms a helix, and tryptophan residues in combination with histidine geometrically form a binding pocket (AlphaFold identifier AF-J9F1D0-F1, model confidence: very high (pLDDT >90)).[26] Hence, the importance of histidine is visible since, without it, the pocket would remain open (Figure 3b). Replacing other amino acids from WIWHCW with histidine, except for tryptophan at the N-terminus, leads to an increase in the fluorescent signal, i.e., stronger binding between the ionomer and the peptide. In the initial random library, histidine is present with a probability of 5/20 in a single sequence, i.e., in >13000 peptides. But it is precisely this combination with tryptophan that ensures stronger binding of the ionomer.
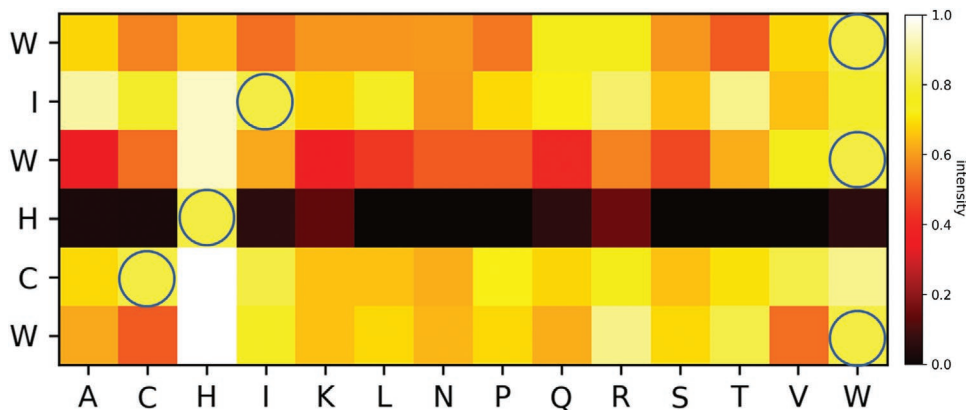
Figure 2. Substitutional analysis of the selective binder WIWHCW. Each pixel represents a peptide sequence where one of the amino acids from the WIWHCW is substituted against the other 14 shown on the horizontal axis. Blue circles indicate the location of the initial WIWHCW on the chip. The amino acid His is essential for selective binding. The intensity of the signal is given in arbitrary units.
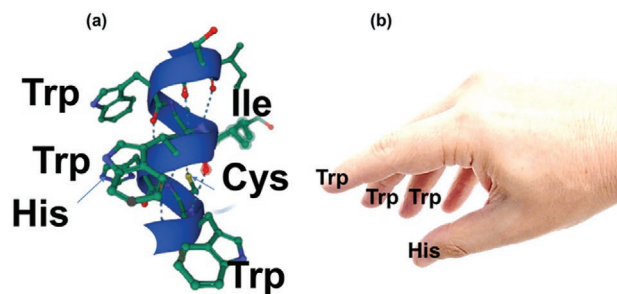
Figure 3. Structure of the selective binding pocket of WIWHCW. a) Helix structure of the peptide WIWHCW. b) Schematic presentation of the selective binding geometry as a gripping hand with Trp (W) and His (H) side chains as fingers.

The helix structure of the peptide indicates the importance of the geometric proximity of Trp and His for the selective binding of the ionomer. The interaction of the amino acids Trp and His (whose side chains are imidazole and indole, respectively) performs several important biochemical functions. The protonation of His37 and concomitant cation-π interaction with Trp41 is a key step in activating the M2 ion channel from the influenza virus.[27] The proton transfer was observed across the NH−N hydrogen bond between the indole and imidazole side chains of Trp and His dimers embedded in helium droplets.[28]

The electrical properties of the peptide as a template do not play an important role. However, the potential proton conductivity of WIWHCW could be related to specific binding mechanisms between the peptide and Nafion.

We plotted the intensity of the fluorescent signal for ten substitutional peptide variants of WIWHCW with the highest fluorescence intensities (black dots with error bars, see **Figure 4**). To estimate the equilibrium dissociation constant K_D, these signals were approximated by saturation curves (red solid curves) according to the formula:[29]

$$I_{obs} = I_{sat} \frac{N}{K_D + N} \qquad (1)$$

where I_{sat} is the maximum fluorescent signal at saturation, and N is the concentration of the analyte (ionomer in our case) in the solution. The corresponding values of the dissociation constants are presented in the inlets of Figure 4. The dissociation constants of the strongest peptide binders are of the same order of magnitude and are in the range of hundred micromolar ($K_D = 140$ µM, SR = 0.37 for WIWHCW). Thus, the selective binding of the peptide binders to Nafion is significantly weaker than the average affinity of antibodies to antigens ($\approx$10 nM) but is in the range of most protein-protein interactions in the cell.[30]
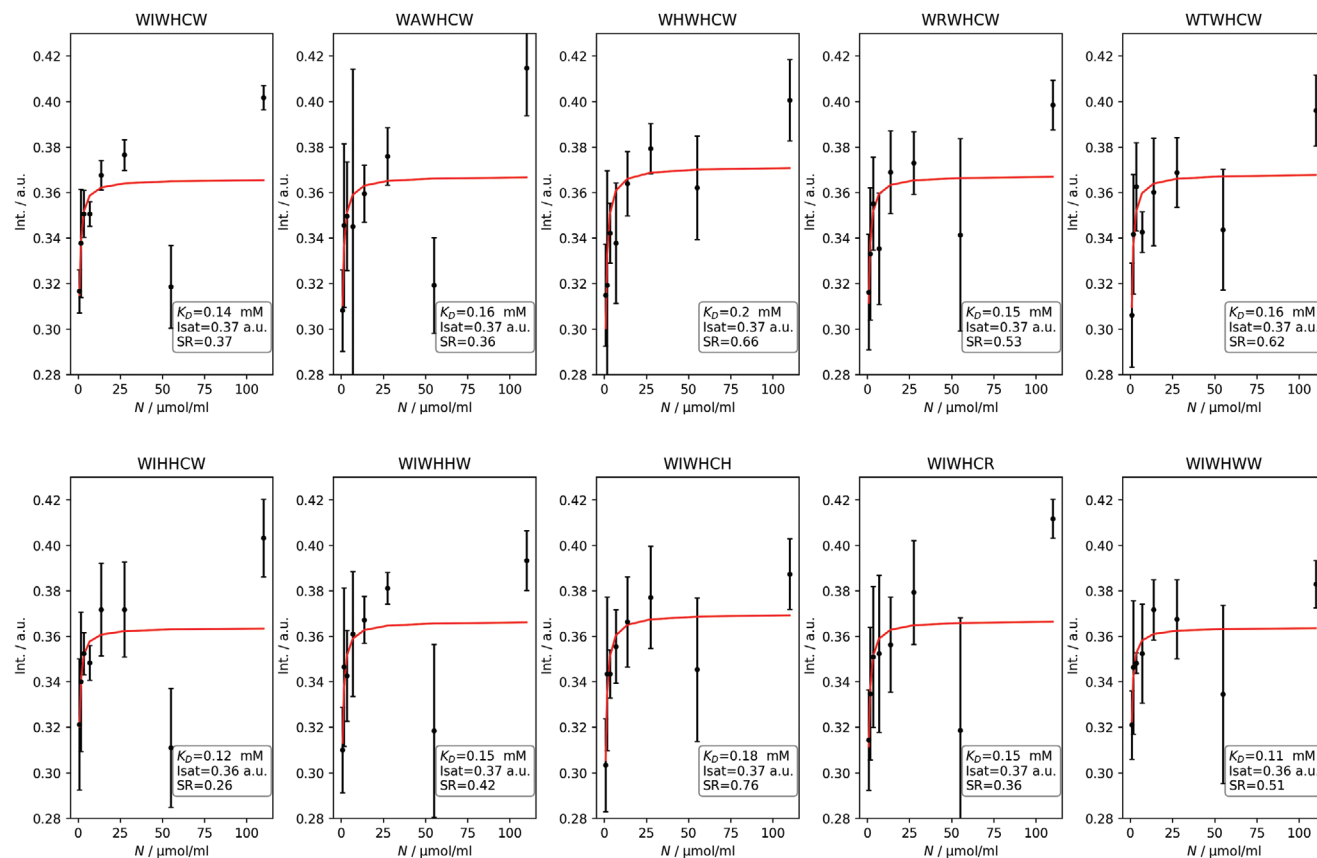
Figure 4. Fluorescence intensity (Int.) of the peptide spots for ten different peptides versus the different Nafion ionomer concentrations in ethanol. The signals (black dots with standard deviations) were fitted with the saturation curve (red line) according to the formula (1). An equilibrium dissociation constant KD of 140 µM (SR = 0.37) was obtained for the peptide WIWHCW.

**ADVANCED
SCIENCE NEWS**

www.advancedsciencenews.com

**ADVANCED
FUNCTIONAL
MATERIALS**

www.afm-journal.de

Fitting saturation curves for fluorescent signals was not very effective, given that values of the approximation parameter SR varied from 0.26 to 0.76 (inlet in Figure 4). This indicates that there were additional effects in the saturation region that statistical error cannot explain. Studies of antibody aggregation on peptide spots have already reported variations in fluorescent signals on saturation curves.[25] The variations of the saturated signals were associated with a mutual interaction of the dye molecules with an increase in their concentration on the spots.

Nafion has a fluorescence spectrum depending on the solvent.[31] However, the mechanisms of such autofluorescence are complex and not fully elucidated. From the point of view of improving detection, other label-free methods are also possible, for example, the more time-consuming but more reliable Time-of-Flight Secondary Ion Mass Spectrometry SIMS (ToF SIMS imaging) that is very sensitive to the organic molecule fragments with fluorine or sulfur[32] (both present in Nafion). The profiles of the ionomer films accumulated on the peptide spots were measured using label-free vertical scanning interferometry (Figure 1d). The significant variation in the Nafion profile within the peptide spots could be related to the variation in the polymer layer on which the peptides were synthesized.

2.3. NMR Validation of Nafion-Peptide Binding

The binding of Cy5-WIWHCW to Nafion creates a bound complex with a longer correlation time than the unbound peptide—leading to faster relaxation and line broadening in nuclear magnetic resonance.[33] This effect is shown in **Figure 5**, where we have titrated a peptide solution with a 1/4 vol/vol solution of Nafion PFSA D2020CS/methanol-d4. Upon the addition of Nafion, substantial line broadening is visible in the aromatic
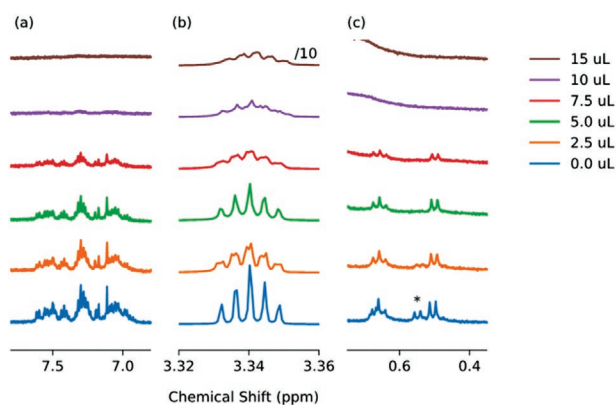
Figure 5. Titration of Cy5-WIWHCW with a 1/4 vol/vol Nafion/Methanol-d4 solution. Panels (a), (b), and (c) show the aromatic region of the 1H spectrum near 7 ppm, the residual solvent signal at 3.34 ppm, and methyl signals of isoleucine near 0.5 ppm, respectively. Adding the 1/4 vol/vol Nafion/Methanol-d4 solution leads to significant broadening in the aromatic and methyl regions of the peptide spectrum. The broadening of the solvent signal in panel (b) is insignificant by comparison. Note that panels (a) and (c) span a chemical shift range of the order of 0.4 ppm, whereas panel (b) spans a ten times smaller range. Spectra are offset vertically for clarity.

region (panel a) and the methyl region (panel c). The two doublets near 0.5 ppm are attributed to the methyl groups of Ile, although isoleucine is not an invariant amino acid in selective binding to the ionomer (Figure 2). One indeed expects all peptide signals to broaden due to the overall change of the peptide's correlation time upon binding to Nafion. The downfield doublet (indicated with an asterisk) shows stronger line-broadening than the upfield one, which we attribute to the different rotational correlation times of the two methyl groups.

Note that paramagnetic impurities may also cause line-broadening. However, the residual solvent signal of mono-protonated methyl groups in CD3OD, shown in Figure 5b) shows only very weak broadening (note the different chemical shift ranges of panels a) and c) on the one hand, and b) on the other). Paramagnetic impurities are also unlikely to cause differential line broadening as we observe here.

It is possible to observe the complex formation using ¹⁹F NMR. However, the ¹⁹F signals of Nafion are very broad due to the size dispersion of the Nafion polymer and the substantial chemical shift anisotropy of ¹⁹F.[34]

2.4. Peptide Interactions with Nafion Membrane

Nafion N212 membrane (Fuel Cell Store, Pinon Drive, TX, USA) was placed on a glass microscope slide and fixed in the incubation tray shown in Figure 1a instead of the peptide chip. This enabled the incubation of different peptides in tray wells and the comparison of their adhesion on the film surface. The adhesion of AWIWHCW peptide and HA epitope AYPYDVPDY (PSL GmbH, Heidelberg, Germany) was studied. HA epitope was used as a control peptide since no ionomer adhesion was observed in Nafion dispersion experiments. Fluorescent dye Cy5 was attached to the peptides through the N-terminal of the amino acid alanine (A) to characterize peptide adhesion optically. Both peptides were dissolved with a 12,5 µg mL⁻¹ concentration in a 50:50 methanol-water solution and incubated in tray wells. We limited the incubation time to 15 min since a long time leads to significant swelling of the Nafion film. After incubation, the solutions with peptides were washed off with distilled water. The intensities of the fluorescent signals I_p of the adherent peptides normalized to the autofluorescence intensity I_f of the Nafion membrane are shown in **Figure 6**. Even with a limited incubation time, at which saturation was not reached, a difference in fluorescent intensity was observed between the selective binder and the control peptide. An I_p/I_f ratio greater than one for the control peptide could be caused by weak adhesion of the fluorescent dye Cy5 to the Nafion membrane. Thus, a significant contribution of the dye to the binding of the WIWHCW peptide to the membrane can be excluded.

The availability of functional groups on the surface of the Nafion membrane is determined by its morphology, which is still a matter of study.[35] In the case of adhesion of a selective peptide from a solution (50:50 methanol-water solution in our case, Figure 6), which activates the mechanisms of membrane swelling, the availability of all functional groups of the ionomer on the surface should have increased.

While screening for selective binders was performed with covalently bound peptides in the presence of the ionomer
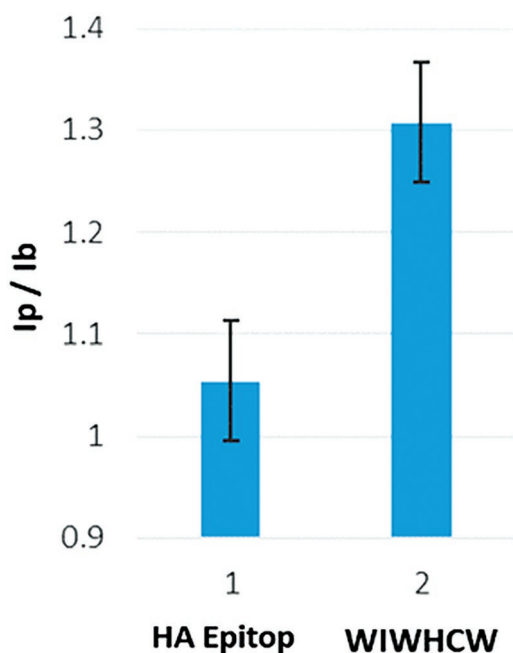
Figure 6. Normalized fluorescence intensity of Nafion membrane after incubating with Cy5-labeled peptides: control HA epitope YPYDVPDY and the selective peptide binder WIWHCW. The intensity was normalized for the autofluorescence of the Nafion membrane.

solution, in this case, on the contrary, selective binding was observed between the Nafion membrane and the peptide solution. This result indicates that the template with immobilized peptides can also selectively bind to the Nafion membrane.

3. Conclusion

We have demonstrated a novel use case for the ultra-high density peptide array: The screening for selective peptide binders to technical polymers using Nafion as an example. A family of selective binders with dissociation constants in the range from 100 to 200 µM was found.

Although we were able to find a selective binder and its variations, the screening was carried out with a relatively small peptide library (56014 different 6-mer peptides, <0.09%) compared to the full combinatorics of 20 canonical amino acids for a sequence with six residues (64 million peptides). To search for potentially stronger binders, it is possible to significantly expand the peptide library if the screening is carried out with a dozen similar peptide arrays (each peptide chip has the format of a standard microscope slide) and their full capacity of a maximum of 200000 spots per peptide array is used. Alternatively, selective affinity can be increased by limiting the entropy of the peptide, for example, by its cyclizing via two cysteine thiol groups and diverse clips.[36] Permutation analysis showed that the Ile position was irrelevant for the specific binding of WIWHCW to Nafion and could be replaced by a second Cys to provide an additional disulfide bridge.

The proposed method allows high-speed screening for selective binders to technical polymers and high-speed validation of screening results. So, for example, in one well of the 16-well tray, up to 6000 spots can be synthesized, i.e., carrying out K_D measurements in parallel for 6000 potential binders, which significantly overperforms all known state-of-the-art techniques for measuring equilibrium binding kinetics on the surface.

Substitution analysis demonstrated a significant role of His in the binding of the ionomer. Adding additional histidine in sequence in the presence of three or two tryptophans increases the binding strength between the peptide and the ionomer.

NMR measurements confirmed the ionomer binding through significant broadening in the aromatic and methyl regions of the peptide spectrum.

A short stable helix can be used to design the ionomer nanostructures via virus-templated synthesis at the peptide level mentioned in the introduction. Given the variety of viral structures with alpha helices on the surface, selective peptide binders to technical polymers may have great potential for designing novel virus-templated materials from the given polymers.

4. Experimental Section

Nafion PFSA Polymer Dispersion: (D2020CS, DuPont Fuel Cells, Wilmington, DE) Components, wt.%: perfluorosulfonic acid/TFE copolymer 20–22, 1-propanol 42–50, water 30–38, ethanol <5, mixed ethers, and other VOCs <2. Total Acid Capacity, H+ polymer basis was 1.03–1.12 meq g^{-1}.

Incubation of Peptide Chips with Nafion Dispersion and Anti-HA-Antibodies: First, the peptide chip (stored at argon) was incubated with PBS-T (PBS containing 0.05% Tween 20 (Sigma Aldrich, St. LouisCity, USA)) for 10 min to regenerate peptide spots. Then, in the case of Nafion dispersion, the peptide chip was incubated with Nafion dispersion diluted as indicated in the results section for 12 h in the dark at room temperature. After that, unbound ionomer molecules were removed by washing the peptide chip with ethanol 3 times for 1 min.

In the case of incubation with anti-HA antibodies (Creative-Diagnostics, NY, USA), the chip was first blocked by Rockland buffer (MB-070, Rockland Immunochemicals, USA) for 10 min. and then washed with PBS-T 3 times for 1 min. The antibodies were incubated in a PBS-T solution at 1 µg mL^{-1} concentration for 1 h in the dark at room temperature. Unbound antibodies were removed by washing the peptide chip with PBS-T 3 times for 1 min.

All incubations were conducted under agitation using an orbital shaker with a rotation speed of 140 rpm. The peptide chips were dried using a compressed air gun.

Image Acquisition: Fluorescence scans of peptide chips were performed with Innoscan 1100 AL (Innopsys, Carbonne, France) with an excitation wavelength of 532 nm (filter set 582 nm/75 nm) with a resolution of 2 µm, speed of 35 µm s^{-1}, and a PMT gain of ten.

Spot topology in Figure 1d,e was imaged by the Contour GT-K by Bruker using Vertical Scanning Interferometry in VXI mode for higher z-resolution at ambient conditions.

Photometric measurements in Figure 6 were performed with Nikon Eclipse Ti-E Inverted Optical Microscope and NIS Elements AR 5.30.04 analysis program (Nikon Plan Fluor 10x/0.75 Ph2 DLL objective, gain: 47,1, exposure time 100 ms). The fluorescence intensity was compared with the free software ImageJ, which allowed for the calculation of mean grey values and their standard deviations over the selected area. The standard deviations in Figure 6 resulted as the sum of standard deviations of corresponding values for fluorescence intensities measured. The standard deviation for the control Ip/If ratio was 0.059, and, for the selective peptide, 0.065, respectively. In Figure 6, they are rounded up to 0.06.

**ADVANCED
SCIENCE NEWS**

www.advancedsciencenews.com

**ADVANCED
FUNCTIONAL
MATERIALS**

www.afm-journal.de

NMR Measurements: ^{1}H NMR spectra were recorded with a 400 MHz spectrometer (Bruker, Karlsruhe, Germany). A 600 micromolar solution of the peptide in methanol-d4 was filled into a 5 mm NMR tube, and the first spectrum was recorded. Then, to ensure thorough mixing, the solution was removed from the NMR tube, mixed with 2.5 µL of the Nafion/Methanol-d4 solution, and filled back into the NMR tube, and the second spectrum was recorded. This procedure was repeated four times. For the fifth addition, the Nafion/methanol-d[4] solution volume was increased to 5 µL. Each spectrum is an average of 32 scans. All spectra were referenced to the residual methanol CHD_2 signal at 3.34 ppm. The data were processed with the home-written package.

Statistical Analysis of Signals from the Dilution Experiment: Each well of the incubation tray contained the same library. Eight wells were used, which were incubated with different polymer concentrations. Each peptide in a separate well was represented by six copies. In Figure 2, the values were taken from a well with a polymer concentration of 0.11 mmol mL^{-1}. The values on the graph resulted from a median for six copies normalized to the background.

Figure 3 contains ten graphs. Each graph consists of eight points with a corresponding standard deviation. The eight points and the corresponding standard deviation were derived from six copies of the corresponding incubation well. The curve fitting was done using the *curve_fit* function from the *scipy* Python library.

Acknowledgements

Conflict of Interest

A.N.-M. is a cofounder of axxelera UG.

Author Contributions

P.G. and A.N-M. conceived the experiments. D.S. conducted incubation experiments and image acquisition and analyzed the results. I.B. analyzed fluorescence signals. J.R., M.B., and T.G. optimized binding kinetics, N.Z. and P.Q. developed Nafion samples for experiments, J.B. synthesized peptides, A.J. and M.S. supported the chemical analysis of results, and P.S. and P.P. conducted NMR experiments. The project was supervised by P.G., A.N.-M., P.S., B.M., W.S., S.B., and G.L.. A.N.-M. wrote the manuscript. All authors discussed the results and commented on the manuscript.

Data Availability Statement

The data that support the findings of this study are available from the corresponding author upon reasonable request.

Keywords

[1] a) I. Staffell, D. Scamman, A. V. Abad, P. Balcombe, P. E. Dodds, P. Ekins, N. Shah, K. R. Ward, *Environ. Sci.* **2019**, *12*, 463; b) K. Itaoka, A. Saito, K. Sasaki, *Int. J. Hydrogen Energy* **2017**, *42*, 7290.

[2] a) S. M. Andersen, M. Borghei, P. Lund, Y. R. Elina, A. Pasanen, E. Kauppinen, V. Ruiz, P. Kauranen, E. M. Skou, *Solid State Ionics* **2013**, *231*, 94; b) D. P. He, S. C. Mu, D. Pan, *Carbon* **2011**, *49*, 82.

[3] X. X. Zhang, D. Trieu, D. Zheng, W. X. Ji, H. N. Qu, T. Y. Ding, D. T. Qiu, D. Y. Qu, *Ind. Eng. Chem. Res.* **2021**, *60*, 11086.

[4] a) J. H. Jung, M. S. Cha, J. B. Kim, *J Nanosci. Nanotechnol.* **2012**, *12*, 5412; b) S. M. Andersen, M. Borghei, R. Dhiman, H. Jiang, V. Ruiz, E. Kauppinen, E. Skou, *Carbon* **2014**, *71*, 218.

[5] a) M. F. Li, Z. P. Zhao, T. Cheng, A. Fortunelli, C. Y. Chen, R. Yu, Q. H. Zhang, L. Gu, B. V. Merinov, Z. Y. Lin, E. B. Zhu, T. Yu, Q. Y. Jia, J. H. Guo, L. Zhang, W. A. Goddard, Y. Huang, X. F. Duan, *Science* **2016**, *354*, 1414; b) X. L. Tian, X. Zhao, Y. Q. Su, L. J. Wang, H. M. Wang, D. Dang, B. Chi, H. F. Liu, E. J. M. Hensen, X. W. Lou, B. Y. Xia, *Science* **2019**, *366*, 850.

[6] K. Jiao, J. Xuan, Q. Du, Z. M. Bao, B. A. Xie, B. W. Wang, Y. Zhao, L. H. Fan, H. Z. Wang, Z. J. Hou, S. Huo, N. P. Brandon, Y. Yin, M. D. Guiver, *Nature* **2021**, *595*, 361.

[7] X. Liu, Y. Li, J. D. Xue, W. K. Zhu, J. F. Zhang, Y. Yin, Y. Z. Qin, K. Jiao, Q. Du, B. W. Cheng, X. P. Zhuang, J. X. Li, M. D. Guiver, *Nat. Commun.* **2019**, E10.

[8] K. T. Nam, D. W. Kim, P. J. Yoo, C. Y. Chiang, N. Meethong, P. T. Hammond, Y. M. Chiang, A. M. Belcher, *Science* **2006**, *312*, 885.

[9] O. N. Antonescu, A. Rasmussen, N. A. M. Damm, D. F. Heidemann, R. Popov, A. Nesterov-Mueller, K. E. Johansson, J. R. Winther, *PLoS One* **2021**, 16.

[10] L. Adler-Abramovich, E. Gazit, *Chem. Soc. Rev.* **2014**, *43*, 6881.

[11] S. Kim, J. H. Kim, J. S. Lee, C. B. Park, *Small* **2015**, *11*, 3623.

[12] a) F. F. Loeffler, T. C. Foertsch, R. Popov, D. S. Mattes, M. Schlageter, M. Sedlmayr, B. Ridder, F. X. Dang, C. von Bojnicic-Kninski, L. K. Weber, A. Fischer, J. Greifenstein, V. Bykovskaya, I. Buliev, F. R. Bischoff, L. Hahn, M. A. R. Meier, S. Brase, A. K. Powell, T. S. Balaban, F. Breitling, A. Nesterov-Mueller, *Nat. Commun.* **2016**, 7; b) F. Loeffler, C. Schirwitz, J. Wagner, K. Koenig, F. Maerkle, G. Torralba, M. Hausmann, F. R. Bischoff, A. Nesterov-Mueller, F. Breitling, *Adv. Funct. Mater.* **2012**, *22*, 2503.

[13] A. Jeihanipour, J. Lahann, *Adv. Mater.* **2022**, *34*, 2110404.

[14] Z. H. Su, N. Pramounmat, S. T. Watson, J. N. Renner, *Soft Matter* **2018**, *14*, 3528.

[15] S. Brown, *Nat. Biotechnol.* **1997**, *15*, 269.

[16] S. R. Whaley, D. S. English, E. L. Hu, P. F. Barbara, A. M. Belcher, *Nature* **2000**, *405*, 665.

[17] G. P. Smith, *Science* **1985**, *228*, 1315.

[18] M. Y. He, M. J. Taussig, *Nat. Methods* **2007**, *4*, 281.

[19] J. Yamaguchi, M. Naimuddin, M. Biyani, T. Sasaki, M. Machida, T. Kubo, T. Funatsu, Y. Husimi, N. Nemoto, *Nucleic Acids Res.* **2009**, *37*, e108.

[20] N. Zambrano, G. Froechlich, D. Lazarevic, M. Passariello, A. Nicosia, C. De Lorenzo, M. J. Morelli, E. Sasso, *Cancers* **2022**, *14*, 1325.

[21] K. A. Mauritz, R. B. Moore, *Chem. Rev.* **2004**, *104*, 4535.

[22] S. M. Andersen, M. Borghei, R. Dhiman, V. Ruiz, E. Kauppinen, E. Skou, *J. Phys. Chem. C* **2014**, *118*, 10814.

[23] F. Jenne, S. Biniaminov, N. Biniaminov, P. Marquardt, C. Von Bojnicic-Kninski, R. Popov, A. Seckinger, D. Hose, A. Nesterov-Mueller, *Int. J. Mol. Sci.* **2022**, *23*, 3515.

[24] A. Bateman, M. J. Martin, S. Orchard, M. Magrane, S. Ahmad, E. Alpi, E. H. Bowler-Barnett, R. Britto, A. Cukura, P. Denny, T. Dogan, T. Ebenezer, J. Fan, P. Garmiri, L. J. D. Gonzales, E. Hatton-Ellis, A. Hussein, A. Ignatchenko, G. Insana, R. Ishtiaq, V. Joshi, D. Jyothi, S. Kandasaamy, A. Lock, A. Luciani, M. Lugaric, J. Luo, Y. Lussi, A. MacDougall, F. Madeira, et al., *Nucleic Acids Res.* **2022**, *51*, D523.

[25] A. Palermo, R. Thelen, L. K. Weber, T. Foertsch, S. Rentschler, V. Hackert, J. Syurik, A. Nesterov-Mueller, *High Throughput* **2019**, *8*, 7.

[26] J. Jumper, R. Evans, A. Pritzel, T. Green, M. Figurnov, O. Ronneberger, K. Tunyasuvunakool, R. Bates, A. Zidek, A. Potapenko, A. Bridgland, C. Meyer, S. A. A. Kohl, A. J. Ballard, A. Cowie, B. Romera-Paredes, S. Nikolov, R. Jain, J. Adler, T. Back, S. Petersen, D. Reiman, E. Clancy, M. Zielinski, M. Steinegger, M. Pacholska, T. Berghammer, S. Bodenstein, D. Silver, O. Vinyals, et al., *Nature* **2021**, *596*, 583.

[27] A. Okada, T. Miura, H. Takeuchi, *Biochemistry* **2001**, *40*, 6053.

[28] B. Bellina, D. J. Merthe, V. V. Kresin, *J. Chem. Phys.* **2015**, *142*, 114306.

[29] R. B. Jones, A. Gordus, J. A. Krall, G. MacBeath, *Nature* **2006**, *439*, 168.

[30] L. Y. Lian, *Prog. Nucl. Magn. Reson. Spectrosc.* **2013**, *71*, 59.

[31] N. F. Bunkin, A. V. Shkirin, V. A. Kozlov, B. W. Ninham, E. V. Uspenskaya, S. V. Gudkov, *J. Chem. Phys.* **2018**, *149*, 164901.

[32] B. Muenster, A. Welle, B. Ridder, D. Althuon, J. Striffler, T. C. Foertsch, L. Hahn, R. Thelen, V. Stadler, A. Nesterov-Mueller, F. Breitling, F. F. Loeffler, *Appl. Surf. Sci.* **2016**, *360*, 306.

[33] A. D. Gossert, W. Jahnke, *Prog. Nucl. Magn. Reson. Spectrosc.* **2016**, *97*, 82.

[34] M. Yamaguchi, T. Matsunaga, K. Amemiya, A. Ohira, N. Hasegawa, K. Shinohara, M. Ando, T. Yoshida, *J. Phys. Chem. B* **2014**, *118*, 5752.

[35] a) K. D. Kreuer, G. Portale, *Adv. Funct. Mater.* **2013**, *23*, 5390; b) J. A. Elliott, D. S. Wu, S. J. Paddison, R. B. Moore, *Soft Matter* **2011**, *7*, 6820.

[36] Z. Dekan, M. Mobli, M. W. Pennington, E. Fung, E. Nemeth, P. F. Alewood, *Angew. Chem., Int. Ed.* **2014**, *53*, 2931.